Distribution and characteristic of nitrite-dependent anaerobic methane oxidation bacteria in wastewater treatment plants and agriculture fields in northern China

Zhen Hu Corresp., [1] , **Ru Ma** [1]

[1] School of Environmental Science and Engineering, Shandong University, Jinan, China

Corresponding Author: Zhen Hu
Email address: huzhen885@sdu.edu.cn

Nitrite-dependent anaerobic methane oxidation (n-damo) is a recently discovered biological process, which has been arousing global attention because of its potential in minimizing greenhouse gases emissions. In this study, molecular biological techniques and potential n-damo activity batch experiments were conducted to investigate the presence and diversity of *M. oxyfera* bacteria in paddy field, corn field, and wastewater treatment plant (WWTP) of northern China, as well as lab-scale n-damo enrichment culture. N-damo enrichment culture showed the highest abundance of *M. oxyfera* bacteria and positive correlation was observed between potential n-damo rate and abundance of *M. oxyfera* bacteria. Both paddy field and corn field were believed to be better inoculum than WWTP for the enrichment of *M. oxyfera* bacteria, due to their higher abundance and diversity of *M. oxyfera* bacteria. Comparative analysis revealed that long biomass retention time, low NH_4^+ and high NO_2^- content were suitable for the growth of *M. oxyfera* bacteria.

Distribution and characteristic of nitrite-dependent anaerobic methane oxidation bacteria by comparative analysis of wastewater treatment plants and agriculture fields in northern China

Zhen Hu[a,*], Ru Ma [a]

[a] School of Environmental Science and Engineering, Shandong University, Jinan, Shandong, China.

Corresponding Author:

Zhen Hu

No. 27 Shanda South Road, Jinan, Shandong 250100,China

E-mail: huzhen885@sdu.edu.cn

10 **Introduction**

11 Methane (CH_4) and nitrous oxide (N_2O) are important greenhouse gases, accounting for about 20% and 7% of
12 global warming, respectively (Griggs & Noguer 2002; Knittel & Boetius 2009). Cai (2012) reported that
13 anthropogenic activities, rather than natural sources, are the major sources of CH_4 and N_2O emissions. And it
14 is widely accepted that wastewater treatment plants (WWTPs) and agricultural fields are two of the most
15 important anthropogenic GHGs sources (Foley et al. 2011; Liu et al. 2014a). In WWTPs, enormous amount of
16 CH_4 and N_2O would be produced during the biological transformation of carbohydrates and nitrogenous
17 compounds, respectively. Our previous on-site investigation showed that about 4.48-9.68×10^9 g of CH_4 and
18 0.93-1.28×10^9 g of N_2O would be emitted from WWTPs of China per year (Wang et al. 2011a; Wang et al.
19 2011b). And compared with WWTPs, agricultural field was believed to be more important GHGs sources,
20 mainly because the widely usage of chemical fertilizers to improve the productivity (IPCC, 2001). It is
21 reported that agriculture field would contribute to 60% of N_2O and 50% of CH_4 emissions on a global scale
22 (Montzka et al. 2011; Syakila & Kroeze 2011).

23 Anaerobic methane oxidation (AMO) is a recently discovered sink of methane on earth, with a
24 consumption rate of approximately 70-300 Tg CH_4 $year^{-1}$ globally (Cui et al. 2015; Hu et al. 2011). Besides
25 AMO coupled to reduction of sulfate (Timmers et al, 2015; Bian et al. 2001), humic compound (Smemo &

Yavitt 2007), iron (Beal et al. 2009; Segarra et al. 2013) and manganese (Egger et al. 2015), the coupling of AOM to nitrite reduction process, named as nitrite-dependent anaerobic methane oxidation (n-damo), has also been demonstrated (Raghoebarsing et al. 2006). N-damo process is performed by "*Candidatus* Methylomirabilis oxyfera" (*M. oxyfera*) bacteria, which is affiliated with the NC10 phylum (Ettwig et al. 2010). N-damo process established a unique relationship between carbon cycle and nitrogen cycle (Raghoebarsing et al. 2006), and it was believed to be a promising method to minimize greenhouse gases emissions through converting CH_4 and N_2O to CO_2 and N_2, respectively (Raghoebarsing et al. 2006; Shen et al. 2015).

Presently, many studies have focused on the distribution *of M. oxyfera* bacteria in natural environment, e.g., freshwater lakes (Liu et al. 2014b), paddy soil (Wang et al. 2012), marine sediments (Chen et al. 2014), wetlands (Hu et al. 2014b), and etc. However, to date, information about distribution of *M. oxyfera* bacteria in northern China is still lacking. In addition, various inoculums have been reported to be able to enrich *M. oxyfera* bacteria successfully, including freshwater sediment (Raghoebarsing et al. 2006), sewage treatment sludge (Luesken et al. 2011a), ditch sediments (Ettwig et al. 2009) and paddy soil (Shen et al. 2014a; Wang et al. 2012). He et al. (2014) found that inoculum sources had significant effect on enrichment of *M. oxyfera* bacteria, and claimed that paddy soil was the optimal inoculum. However, intensive study on inoculum sources from the perspective of microorganism is absence.

In this study, the presence and diversity of *M. oxyfera* bacteria in four different sites of northern China, i.e., paddy field, corn field, WWTP and n-damo enrichment culture, were investigated through molecular biological techniques and potential n-damo activity batch experiments. Comparative analysis of environmental features and *M. oxyfera* bacteria activity was conducted to reveal the characteristics of *M. oxyfera* bacteria, as well as its optimal growth conditions.

Materials and methods

Site description and sample collection

Non-flooded paddy field with rice reaping once per year (PF) and corn field with maize-wheat rotation for over 50 years (CF), both of which are typical agricultural type of northern China, were selected as agricultural field sample sites. PF cores and CF cores were collected from three locations (5m distance) at the 50-60cm depth in each sampling site, according to the previously described methods (Hu et al. 2014b). Sludge from anaerobic tank of local WWTP (Everbright Water, Jinan China) (WS), and lab-scale Upflow Anaerobic Sludge Bed reactor (UASB) aiming at enrichment of *M.oxyfera* bacteria (EC), were selected as WWTP samples. The sample collection was conducted in October, 2015, and the environmental characteristics of each sample site are listed in Table 1.

All collected samples were placed in hermetic containers and immediately transported to the laboratory

within 4h. Subsequently, the collected samples were equally divided into three parts. The first part was placed in the incubator to measure the potential n-damo activity, the second parts was stored in refrigerator at 4℃ for analysis of physicochemical parameters, and the last part was stored in refrigerator at -20℃ for further microbiological analysis.

Table 1. *Environmental characteristics of the sample sites.*

Physicochemical parameters analysis

Soil samples were extracted with 1M KCl and the concentrations of ammonium, nitrite and nitrate were measured as described by Ryan et al. (2007). Soil pH was measured at soil/water ratio of 1:2.5 using a pH analyzer (HQ30d 53LEDTM, HACH, USA) (Wang et al. 2012). Temperature and salinity of soil was measured in *situ* using HI98331 soil electrical conductivity meter (HI98331, HANNA, Shanghai).

Concentrations of ammonium, nitrite and nitrate in water samples were analyzed according to the standard method (APHA, 2005). Water temperature, pH and salinity were measured in *situ* using pH and salinity analyzer (DDBJ-350, Leici, Shanghai). And CH_4 concentration in gas phase was analyzed using gas chromatograph equipped with flame ionization detector (FID–GC) (7890B, Agilent Technologies, USA).

Potential n-damo activity batch experiment

All the samples were washed three times with anaerobic water to remove the residual NO_x^- (NO_2^- and NO_3^-) and organic compounds, and were then transferred to 1L Ar-flushed glass bottles. The slurries were pre-incubated under anoxic conditions at 32±1 ℃ for at least 48 h, in order to let the microbes adapt to the new environment. The bottle was flushed with Ar gas again before the measurement of potential n-damo activity. Two treatment groups were conducted subsequently: (a) CH_4 (blank group), (b) CH_4+NO_2^-(experimental group). The initial CH_4 concentrations in both blank and experimental groups were 1.02±0.06 mmol L^{-1} and the initial concentrations of NO_2^- in the experimental groups were 0.35±0.01 mmol NO_2^- L^{-1}. The variation of CH_4 and NO_2^- concentrations were determined at intervals of 6 hours. The potential methane oxidation rates and the ratio of CH_4/NO_2^- were evaluated by linear regression of CH_4 and NO_2^- decrease in the experimental groups.

Fluorescence in situ hybridization (FISH)

Approximately 0.3g of collected samples were washed in phosphate-buffered saline (PBS; 10 mM Na_2HPO_4/NaH_2PO_4 pH 7.5 and 130 mM NaCl) and fixed with 4% (w/v) paraformaldehyde in PBS for 3h under 4℃. After incubation, the sediment (fixed biomass) was washed with PBS and then stored in mixture (1ml) of ethanol and PBS (1×) at −20 °C until analysis.

Bacterial probe S-*-DBACT-1027-a-A-18 (5'-TCTCCACGCTCCCTTGCG-3') (Cy3, red), specific for bacteria affiliated with the NC10 phylum were used in this study (Raghoebarsing et al. 2006); and a mixture of

EUB I-III (FITC, green) was used for the detection of total bacteria (Daims et al. 1999). Fixed biomass (10 μl) was spotted on microscopic slides circles and then dehydrated subsequently with 50%, 80%, and 98% of ethanol for 3 min each. The probes were hybridized for 2 h at 46 °C in hybridization buffer (5M NaCl, 1M Tris/HCl pH 8.0, 10% sodium dodecyl sulfate) and 40% formamide. Hybridized samples were washed with hybridization leachate at 48℃ and then added with the fluorescence decay resistance agent. Fluorescence microscope (BX53, Olympus, Japan) was used to observe the prepared slides and the picture was disposed with Image-Pro Plus 6.0.

DNA extraction and PCR amplification

Total DNA was extracted using Power Soil DNA Isolation kit (Mo Bio Laboratories, Carlsbad, CA) according to the manufacturer's protocols. And DNA concentration was measured at 260 nm with Nano-drop spectrophotometer (NanoDrop 1000, Nano-Drop Technologies, USA).

To understand the biodiversity of *M. oxyfera* bacteria, 16S rRNA gene of *M. oxyfera* bacteria was amplified using nested PCR protocols, as previously described (Hu et al. 2014b; In nested PCR, products of the first round PCR were then used as the DNA templates in the following round PCR. For 16S rRNA gene amplification, specific forward primer 202F (Ettwig et al. 2009) and general bacterial reverse primer 1545R (Juretschko et al. 1998) were used for the first round PCR, NC10 specific primers qP1F and qP2R (Ettwig et

106 al. 2009) were performed for the second round PCR. The detailed information of nested PCR is shown in
107 Table S1.

108 ***Quantitative Real-Time PCR (qPCR)***

109 The quantitative PCR of *M. oxyfera* bacteria 16S rRNA gene were performed on LightCycler480 with
110 Sequence Detection Software v1.4 (Applied Biosystems, Life Technologies Corporation, USA). The
111 abundance of 16S rRNA gene was determined using the primers qp1R-qp1F (Ettwig et al. 2009) with 10 μL
112 of Power SYBR Green PCR Master Mix, 1 μL of template DNA (5–20 ng μL^{-1}), 0.4 μL of each primer and
113 8.2 μL of ddH_2O. Detailed information is exhibited in Table S1. Negative-control reactions in which the
114 DNA template was replaced by nuclease-free water were also performed. The whole process was performed
115 under sterile conditions on ice and away from light. Triplicate qPCR analyses were performed for each
116 sample. The standard curve was constructed from purified plasmid DNA with the concentrations ranging
117 from 1.0×10^1 to 1.0×10^7 copies μL^{-1}, and it showed correlation between the DNA template concentration
118 and the crossing point with coefficients of determination ($R^2>0.97$). The qPCR amplification efficiency of the
119 standard curve and reactions were both greater than 85%.

120 ***High-throughput pyrosequencing and data analysis***

After amplification, the purified nested PCR products of 16S rRNA gene were used for pyrosequencing on the Roche 454 GS-FLX Titanium sequencer (Roche 454 Life Sciences, Branford, CT, USA) at Personalbio (Shanghai Personal Biotechnology, Co., Ltd., Shanghai, China).

After pyrosequencing, all the raw reads were analyzed using QIIME standard pipeline (Shu et al. 2015), to trim off the low quality reads, adaptors, barcodes and primers. Then sequences containing ambiguous base calls (Ns) and sequences shorter than 150 bp were also removed. The remaining sequences were clustered into operational taxonomic unites (OTUs) by UCLUST, with identity of 97% (Edgar et al. 2011). The sequences with highest relative abundance in each OUT were annotated with NCBI taxonomy using BLASTN and the Green genes database. Chao1 richness estimator, ACE estimator, Simpson diversity and Good's coverage were calculated in Mothur analysis (http://www.mothur.org). Beta diversity statistics, including cluster analysis, weighted UniFrac distance metrics, and Principal coordinate analysis (PCoA), were conducted based on UniFrac metric (Zhang et al., 2011).

Ethical Statement This article does not contain any studies with human participants or animals performed by any of the authors.

Results

136 ***Physicochemical Characteristics of the Sample Sites***

137 Significant differences in physicochemical characteristics among different environmental samples were
138 observed in the present study. The peak NH_4^+-N content (815.88 mg N kg^{-1} dry sediment) was detected in WS,
139 which was over 80-folds higher than that in the other three sample sites. And the highest NO_2^- -N content
140 (14120 mg N kg^{-1} dry sediment) was observed in EC, while NO_2^- -N content in the other three sample site
141 varied form 0.37-127.19 mg N kg^{-1} dry sediment. Mainly because of its high NO_2^- content, the highest NO_x^--N
142 content was also observed in EC, which was beyond 17-folds higher than that of the other three sample sites. In
143 addition, compared with published researches conducted in paddy fields, where NO_X^--N content was around
144 1.4 -3.3 mg N kg^{-1} dry sediment (Shen et al. 2014a; Zhou et al. 2014 ; Ding et al. 2015), higher NO_X^--N
145 content in the agriculture field (PF and CF) of northern China was observed in this study, mainly caused by
146 difference in farming methods.

147 ***Abundance of M.oxyfera bacteria***

148 FISH analysis was used to investigate the spatial distribution and relative quantification of *M. oxyfera* bacteria
149 compared to total bacteria. As shown in Fig. 1, *M. oxyfera* bacteria (represented by red color) were observed in
150 all four sample sites, and the proportion of *M. oxyfera* bacteria to total bacteria followed the order of

EC>PF>CF>WS. Notably, compared with total bacteria, *M.oxyfera* bacteria in the enrichment culture took up over 50%, indicating the predominance of *M.oxyfera* bacteria.

To further accurately quantify the abundance of *M. oxyfera* bacteria, qPCR analysis was conducted and significant difference was also observed in different sampling sites. The abundance of *M. oxyfera* bacteria were $7.28\pm0.8\times10^{7}$,$1.55\pm0.3\times10^{7}$, $1.07\pm0.3\times10^{10}$, $2.61\pm0.1\times10^{6}$ copies per gram of dry sediment in PF, CF, EC and WS, respectively (Fig.2). This order was in consistence with results of FISH analysis.

Fig. 1 *FISH image of the collected samples. The M. oxyfera bacteria was hybridized with probe S-*-DBACT-1027-a-A-18(Cy3, red) and total bacteria was hybridized with probes EUB I-III (FITC, green). a&e, PF; b&f, CF; c&g, EC, d&h, WS. The scale bar indicates 100 μm.*

Fig. 2 *The abundance of M. oxyfera bacteria in different sample sites.*

Potential Rates of n-damo Activity

In order to estimate the activity of *M. oxyfera* bacteria, batch experiments were conducted using the collected samples, and the results are shown in Fig. 3. In experimental groups amended with CH_4 and NO_2^-, dramatic decline in CH_4 concentration were observed compared with the blank groups, indicating that CH_4 oxidation was propelled by NO_2^- reduction under anoxic conditions. The detected anaerobic methane oxidizing rates were 3.90 ± 0.05, 2.58 ± 0.08, 22.31 ± 0.02 and 1.61 ± 0.01 μmol CH_4 g^{-1} d^{-1} in PF, CF, EC and WS, respectively. The stoichiometric ratio for methane to nitrite, calculated through the curve fitting method, were 3:5.7 for PF,

168 3:4.6 for CF, 3:6.9 for EC, and 3:3.2 for WS. The value of n-damo enrichment culture was the closest to the
169 theoretical stoichiometric ratio, which was 3:8 (Ettwig et al. 2010).

170 ***Fig. 3*** *The consumption rates of methane and nitrite in the paddy field (a), corn field (b), n-damo enrichment culture (c), WWTP*
171 *(d).*

172 ***Microbial community structure analysis***

173 In order to determine the microbial community structure of different samples, 454 high-throughput sequencing
174 analysis of 16S rRNA gene was conducted. Raw reads obtained from different samples ranged from 11017 to
175 14814 and the good coverage values varied from 86.48% to 94.70% (Table S2), indicating that these sequences
176 were enough to analyze the microbial community structures. Chao1 estimator, ACE estimator, Shannon index
177 and the numbers of OTUs in four samples followed the same order, which was PF>CF>EC>WS (Table S2).

178 To show the diversity of species among different samples, rarefaction curves were drawn in this study
179 (Fig. S1). Results showed that the rarefaction curves of all samples didn't reach a saturation stage, indicating
180 that these samples had highly diverse microbial communities. PCoA was conducted to investigate the
181 differences in microbial community between different samples, based on unweighted UniFrac distance metrics.
182 Results showed that PF and CF tended to cluster together, while EC and WS were obviously different. The
183 results with maximum variation of 87.59% (PC1) and 8.37% (PC2) were shown in Fig. S2.

184 The difference in microbial community of four samples at the phylum level is shown in Fig. 4. A total of
185 16 phyla were identified and NC10 was the main phylum observed in PF, CF and EC, accounting for 74.4%,
186 92.2% and 65.2% of total microorganism, respectively, while *Armatimonadetes* (formerly candidate division
187 OP10) was the dominant phylum in WS and NC10 phylum only accounted for 7.1% of total microorganism
188 in WS. Since not all NC10 phylum bacteria were defined as *M.oxyfera* bacteria (Ettwig et al., 2009; Wang et
189 al. 2015), for better understanding and analysis the diversity of *M. oxyfera* bacteria in different samples, heat
190 map was conducted at the genera level and the results is shown in Fig. 5. *Candidatus.Methylomirabilis*
191 bacteria, which were proved to be able to complete n-damo process (Ettwig et al. 2010), accounted for 1.00%,
192 1.47%, 1.80% and 0.057% of total microorganism in PF, CF, EC and WS, respectively. All these sequences,
193 which were identified as *Candidatus.Methylomirabilis*, were grouped into 8 (PF), 17 (CF), 9 (EC) and 3 (WS)
194 OTUs at the 97% identity level.

195 ***Fig. 4*** *Composition of microbial community at phylum level in different samples.*

196 ***Fig. 5*** *Richness heat map of the 25 most abundant genera.*

197 **Discussion**

198 In present study, PF, CF, EC and WS in northern China, as previously overlooked sites, were selected to
199 investigate the presence and characteristics of n-damo process. Results showed that EC had the highest

potential n-damo activity, as well as the highest abundance of *M. oxyfera* bacteria. Correlation analysis showed that the potential n-damo rates and the abundance of *M. oxyfera* bacteria followed the same descending order, i.e., EC>PF>CF>WS, indicating positive correlation between the two indexes. Moreover, the potential n-damo rate (22.31±0.02 μ mol CH_4 $g^{-1}d^{-1}$) of EC was higher than that reported in other n-damo enrichment culture (He et al. 2014). This was attributed to the relative higher abundance of *M. oxyfera* bacteria in the present study. The abundance of *M. oxyfera* bacteria in the present study was over 20 times higher than that reported by He et al. (2014), which further verified the positive correlation between the potential n-damo rates and the abundance of *M. oxyfera* bacteria.

WWTP showed lower abundance of *M. oxyfera* bacteria than the other three sample sites, mainly because of its short biomass retention time (13 days), while biomass retention time of other three sample sites was years or even decades of years (Kampman et al. 2014; Weiland BP. 2006). With the doubling time of 1-2 weeks (Ettwig et al. 2009), the growth rate of *M. oxyfera* bacteria is much lower than heterotrophic bacteria, indicating that *M. oxyfera* bacteria might be washed out in WWTP and resulted in lower abundance of *M. oxyfera* bacteria. Another possible reason was that high NH_4^+ content in WWTP, which was unfavorable for the growth of *M. oxyfera* bacteria. Winkler et al. (2015) found that anammox bacteria had advantage over *M. oxyfera* bacteria for nitrite in the presence of excess ammonium. What is more interesting, although WS was used as initial inoculum for EC in this study, the abundance of *M. oxyfera* bacteria in EC was over 4×10^3

217 times higher than that in WS. This was mainly attributed to a combination of low NH_4^+ content and high
218 NO_2^- content during the enrichment period of EC. It was reported that the nitrite affinity constant of *M*
219 *.oxyfera* bacteria was 0.6 g NO_2^-- Nm^{-3}, indicating that high NO_2^- content was more beneficial for the growth
220 of *M .oxyfera* bacteria (Winkler et al. 2015).

221 The distribution and composition of NC10 phylum was determined by 16S rRNA gene sequencing
222 analysis. NC10 phylum detected from PF, CF and EC were significant higher than that in WS, which was
223 mainly attributed to short biomass retention time of WWTP. In addition, it can be seen from the heat map that
224 the abundance of *M. oxyfera* bacteria in different samples followed the order of EC>PF>CF>WS, which was
225 consistence with the result of qPCR. What's more, PF and CF had much higher OTU numbers than WS. Thus,
226 it was believed that PF and CF could be favorable inoculum for the enrichment of *M. oxyfera* bacteria, due to
227 their higher abundance and diversity of *M. oxyfera* bacteria. And it's worth to notice that significant
228 difference existed in microbial community between EC and WS, EC has 6 more OTUs than WS, although
229 WS was used as initial inoculum for EC. This might be caused by the optimum enrichment culture for *M.*
230 *oxyfera* bacteria in EC, i.e., low NH_4^+ and high NO_2^- contents. Besides, the increase in diversity of *M. oxyfera*
231 bacteria would also be attributed to the longer biomass retention time of EC.

232 In conclusion, the present study further expanded our knowledge on distribution and characteristic of *M.*
233 *oxyfera* bacteria in northern China. Comparative analysis found that positive correlation existed between

234 abundance of *M. oxyfera* bacteria and potential n-damo activity rate. In addition, PF and CF were identified as
235 suitable inocula to enrich *M. oxyfera* bacteria. Moreover, long biomass retention time, low NH_4^+ and high NO_2^-
236 contents would benefit the growth of *M. oxyfera* bacteria.

237 **References**

238 APHA. 2005. Standard methods for the examination of water and wastewater. *American Public Health*
239 *Association (APHA): Washington, DC, USA*.
240 Bian L, Hinrichs K-U, Xie T, Brassell SC, Iversen N, Fossing H, Jørgensen BB, and Hayes JM. 2001. Algal
241 and archaeal polyisoprenoids in a recent marine sediment: Molecular isotopic evidence for anaerobic
242 oxidation of methane. Geochemistry, Geophysics, Geosystems 2:n/a-n/a. 10.1029/2000gc000112
243 Cai Z. 2012. Greenhouse gas budget for terrestrial ecosystems in China. *Science China Earth Sciences* 55:173-
244 182. 10.1007/s11430-011-4309-8
245 Chen J, Jiang X-W, and Gu J-D. 2014. Existence of Novel Phylotypes of Nitrite-Dependent Anaerobic
246 Methane-Oxidizing Bacteria in Surface and Subsurface Sediments of the South China Sea.
247 *Geomicrobiology Journal* 32:1-10. 10.1080/01490451.2014.917742
248 Cui M, Ma A, Qi H, Zhuang X, and Zhuang G. 2015. Anaerobic oxidation of methane: an “active” microbial
249 process. *MicrobiologyOpen* 4:1-11. 10.1002/mbo3.232
250 Daims H, Brühl A, Amann R, Schleifer K-H, and Wagner M. 1999. The Domain-specific Probe EUB338 is
251 Insufficient for the Detection of all Bacteria: Development and Evaluation of a more Comprehensive
252 Probe Set. *Systematic and Applied Microbiology* 22:434-444. 10.1016/s0723-2020(99)80053-8
253 Deutzmann JS and Schink B. 2011. Anaerobic oxidation of methane in sediments of Lake Constance, an

254 oligotrophic freshwater lake. Appl Environ Microbiol. p 4429-4436.
255 Ding J, Fu L, Ding ZW, Lu YZ, Cheng SH and Zeng RJ. 2015. "Environmental evaluation of coexistence of
256 denitrifying anaerobic methane-oxidizing archaea and bacteria in a paddy field." Appl Microbiol
257 Biotechnol 100(1): 439-446.
258 Edgar RC, Haas BJ, Clemente JC, Quince C, and Knight R. 2011. UCHIME improves sensitivity and speed of
259 chimera detection. *Bioinformatics* 27:2194-2200.
260 Egger M, Rasigraf O, Sapart CJ, Jilbert T, Jetten MSM, Röckmann T, van der Veen C, Bândă N, Kartal B,
261 Ettwig KF, and Slomp CP. 2015. Iron-Mediated Anaerobic Oxidation of Methane in Brackish Coastal
262 Sediments. Environmental Science & Technology 49:277-283. 10.1021/es503663z
263 Emily J. Beal CHH, Victoria J. Orphan. 2009. Manganese- and Iron-Dependent Marine Methane Oxidation.
264 Ettwig KF, Butler MK, Le Paslier D, Pelletier E, Mangenot S, Kuypers MM, Schreiber F, Dutilh BE, Zedelius
265 J, de Beer D, Gloerich J, Wessels HJ, van Alen T, Luesken F, Wu ML, van de Pas-Schoonen KT, Op
266 den Camp HJ, Janssen-Megens EM, Francoijs KJ, Stunnenberg H, Weissenbach J, Jetten MS, and
267 Strous M. 2010. Nitrite-driven anaerobic methane oxidation by oxygenic bacteria. *Nature* 464:543-
268 548. 10.1038/nature08883
269 Ettwig KF, van Alen T, van de Pas-Schoonen KT, Jetten MSM, and Strous M. 2009. Enrichment and
270 Molecular Detection of Denitrifying Methanotrophic Bacteria of the NC10 Phylum. *Applied and*
271 *Environmental Microbiology* 75:3656-3662. 10.1128/aem.00067-09
272 Foley JA, Ramankutty N, Brauman KA, Cassidy ES, Gerber JS, Johnston M, Mueller ND, O'Connell C, Ray
273 DK, West PC, Balzer C, Bennett EM, Carpenter SR, Hill J, Monfreda C, Polasky S, Rockstrom J,
274 Sheehan J, Siebert S, Tilman D, and Zaks DP. 2011. Solutions for a cultivated planet. *Nature* 478:337-
275 342. 10.1038/nature10452

276 Griggs DJ, and Noguer M. 2002. Climate change 2001: the scientific basis. Contribution of working group I to
277 the third assessment report of the intergovernmental panel on climate change. *Weather* 57:267-269.
278 He Z, Cai C, Shen L, Lou L, Zheng P, Xu X, and Hu B. 2014. Effect of inoculum sources on the enrichment of
279 nitrite-dependent anaerobic methane-oxidizing bacteria. *Appl Microbiol Biotechnol* 99:939-946.
280 10.1007/s00253-014-6033-8
281 He Z, Geng S, Shen L, Lou L, Zheng P, Xu X, and Hu B. 2015. The short- and long-term effects of
282 environmental conditions on anaerobic methane oxidation coupled to nitrite reduction. *Water*
283 *Research* 68:554-562. 10.1016/j.watres.2014.09.055
284 Hu B, He Z, Geng S, Cai C, Lou L, Zheng P, and Xu X. 2014a. Cultivation of nitrite-dependent anaerobic
285 methane-oxidizing bacteria: impact of reactor configuration. *Appl Microbiol Biotechnol* 98:7983-7991.
286 10.1007/s00253-014-5835-z
287 Hu BL, Shen LD, Lian X, Zhu Q, Liu S, Huang Q, He ZF, Geng S, Cheng DQ, Lou LP, Xu XY, Zheng P, and
288 He YF. 2014b. Evidence for nitrite-dependent anaerobic methane oxidation as a previously
289 overlooked microbial methane sink in wetlands. *Proc Natl Acad Sci U S A* 111:4495-4500.
290 10.1073/pnas.1318393111
291 Hu S, Zeng RJ, Keller J, Lant PA, and Yuan Z. 2011. Effect of nitrate and nitrite on the selection of
292 microorganisms in the denitrifying anaerobic methane oxidation process. *Environ Microbiol Rep*
293 3:315-319. 10.1111/j.1758-2229.2010.00227.x
294 Intergovernmental Panel on Climate Change (IPCC), *Third Assessment Report. Working Group I,* Cambridge
295 Univ. Press, New York, 2001.
296 Juretschko S, Timmermann G, Schmid M, Schleifer K-H, Pommerening-Röser A, Koops H-P, and Wagner M.
297 1998. Combined molecular and conventional analyses of nitrifying bacterium diversity in activated

298 sludge: Nitrosococcus mobilis and Nitrospira-like bacteria as dominant populations. *Applied and*
299 *environmental microbiology* 64:3042-3051.
300 Kampman C, Temmink H, Hendrickx TLG, Zeeman G, and Buisman CJN. 2014. Enrichment of denitrifying
301 methanotrophic bacteria from municipal wastewater sludge in a membrane bioreactor at 20°C. *Journal*
302 *of Hazardous Materials* 274:428-435. 10.1016/j.jhazmat.2014.04.031
303 Knittel K, and Boetius A. 2009. Anaerobic Oxidation of Methane: Progress with an Unknown Process.
304 *Annual Review of Microbiology*, 311-334.
305 Liu Y, Cheng X, Lun X, and Sun D. 2014a. CH4 emission and conversion from A2O and SBR processes in
306 full-scale wastewater treatment plants. *Journal of Environmental Sciences* 26:224-230.
307 http://dx.doi.org/10.1016/S1001-0742(13)60401-5
308 Liu Y, Zhang J, Zhao L, Li Y, Yang Y, and Xie S. 2014b. Aerobic and nitrite-dependent methane-oxidizing
309 microorganisms in sediments of freshwater lakes on the Yunnan Plateau. *Appl Microbiol Biotechnol*
310 99:2371-2381. 10.1007/s00253-014-6141-5
311 Luesken FA, van Alen TA, van der Biezen E, Frijters C, Toonen G, Kampman C, Hendrickx TLG, Zeeman G,
312 Temmink H, Strous M, Op den Camp HJM, and Jetten MSM. 2011a. Diversity and enrichment of
313 nitrite-dependent anaerobic methane oxidizing bacteria from wastewater sludge. *Appl Microbiol*
314 *Biotechnol* 92:845-854. 10.1007/s00253-011-3361-9
315 Montzka SA, Dlugokencky EJ, and Butler JH. 2011. Non-CO2 greenhouse gases and climate change. *Nature*
316 476:43-50. 10.1038/nature10322
317 Raghoebarsing AA, Pol A, van de Pas-Schoonen KT, Smolders AJ, Ettwig KF, Rijpstra WI, Schouten S,
318 Damste JS, Op den Camp HJ, Jetten MS, and Strous M. 2006. A microbial consortium couples
319 anaerobic methane oxidation to denitrification. *Nature* 440:918-921. 10.1038/nature04617

320 Ryan J, Estefan G, and Rashid A. 2007. *Soil and plant analysis laboratory manual*: ICARDA.

321 Segarra KEA, Comerford C, Slaughter J, and Joye SB. 2013. Impact of electron acceptor availability on the
322 anaerobic oxidation of methane in coastal freshwater and brackish wetland sediments. Geochimica et
323 Cosmochimica Acta 115:15-30. 10.1016/j.gca.2013.03.029

324 Shen L-d, Liu S, He Z-f, Lian X, Huang Q, He Y-f, Lou L-p, Xu X-y, Zheng P, and Hu B-l. 2015. Depth-
325 specific distribution and importance of nitrite-dependent anaerobic ammonium and methane-oxidising
326 bacteria in an urban wetland. *Soil Biology and Biochemistry* 83:43-51.
327 http://dx.doi.org/10.1016/j.soilbio.2015.01.010

328 Shen L-d, Liu S, Huang Q, Lian X, He Z-f, Geng S, Jin R-c, He Y-f, Lou L-p, and Xu X-y. 2014a. Evidence
329 for the cooccurrence of nitrite-dependent anaerobic ammonium and methane oxidation processes in a
330 flooded paddy field. *Applied and environmental microbiology* 80:7611-7619.

331 Shen L-d, Qun Z, Shuai L, Ping D, Jiang-ning Z, Dong-qing C, Xiang-yang X, Ping Z, and Bao-lan H. 2014b.
332 Molecular evidence for nitrite-dependent anaerobic methane-oxidising bacteria in the Jiaojiang
333 Estuary of the East Sea (China). *Appl Microbiol Biotechnol* 98:5029-5038. 10.1007/s00253-014-5556-
334 3

335 Shu D, He Y, Yue H, Zhu L, and Wang Q. 2015. Metagenomic insights into the effects of volatile fatty acids
336 on microbial community structures and functional genes in organotrophic anammox process.
337 Bioresource Technology 196:621-633. 10.1016/j.biortech.2015.07.107

338 Smemo KA, and Yavitt JB. 2007. Evidence for Anaerobic CH4 Oxidation in Freshwater Peatlands.
339 Geomicrobiology Journal 24:583-597. 10.1080/01490450701672083

340 Syakila A, and Kroeze C. 2011. The global nitrous oxide budget revisited. *Greenhouse Gas Measurement and*
341 *Management* 1:17-26. 10.3763/ghgmm.2010.0007

342 Tamura K, Dudley J, Nei M, and Kumar S. 2007. MEGA4: molecular evolutionary genetics analysis (MEGA)
343 software version 4.0. *Molecular biology and evolution* 24:1596-1599.
344 Timmers PHA, Suarez-Zuluaga DA, van Rossem M, Diender M, Stams AJM, and Plugge CM. 2015.
345 Anaerobic oxidation of methane associated with sulfate reduction in a natural freshwater gas source.
346 *The ISME Journal* 10:1400-1412. 10.1038/ismej.2015.213
347 Wang J, Zhang J, Wang J, Qi P, Ren Y, and Hu Z. 2011a. Nitrous oxide emissions from a typical northern
348 Chinese municipal wastewater treatment plant. *Desalination and Water Treatment* 32:145-152.
349 10.5004/dwt.2011.2691
350 Wang J, Zhang J, Xie H, Qi P, Ren Y, and Hu Z. 2011b. Methane emissions from a full-scale A/A/O
351 wastewater treatment plant. *Bioresource Technology* 102:5479-5485. 10.1016/j.biortech.2010.10.090
352 Wang Y, Zhu G, Harhangi HR, Zhu B, Jetten MSM, Yin C, and Op den Camp HJM. 2012. Co-occurrence and
353 distribution of nitrite-dependent anaerobic ammonium and methane-oxidizing bacteria in a paddy soil.
354 *FEMS Microbiology Letters* 336:79-88. 10.1111/j.1574-6968.2012.02654.x
355 Weiland BP. 2006. Biomass Digestion in Agriculture: A Successful Pathway for the Energy Production and
356 Waste Treatment in Germany. Engineering in Life Sciences 6:302-309. 10.1002/elsc.200620128
357 Winkler MKH, Ettwig KF, Vannecke TPW, Stultiens K, Bogdan A, Kartal B, and Volcke EIP. 2015.
358 Modelling simultaneous anaerobic methane and ammonium removal in a granular sludge reactor.
359 *Water Research* 73:323-331. 10.1016/j.watres.2015.01.039
360 Yan P, Li M, Wei G, Li H, and Gao Z. 2015. Molecular Fingerprint and Dominant Environmental Factors of
361 Nitrite-Dependent Anaerobic Methane-Oxidizing Bacteria in Sediments from the Yellow River
362 Estuary, China. *Plos One* 10:e0137996. 10.1371/journal.pone.0137996
363 Zhang T, Shao, M.-F., Ye, L., 2011. 454 Pyrosequencing reveals bacterial diversity of activated sludge from
364 14 sewage treatment plants. ISME J. 6, 1137–1147.
365 Zhou LL, Wang Y, Long XE, Guo JH, Zhu GB. 2014. "High abundance and diversity of nitrite-dependent

366 anaerobic methane-oxidizing bacteria in a paddy field profile." FEMS Microbiology Letters 360(1):
367 33-41.
368
369

Table 1(on next page)

Environmental characteristics

Environmental characteristics of the sample sites.

1 **Distribution and characteristic of nitrite-dependent anaerobic methane oxidation bacteria in wastewater**

2 **treatment plants and agriculture fields in northern China**

3 **Zhen Hu[a,*], Ru Ma [a]**

4 [a] School of Environmental Science and Engineering, Shandong University, Jinan, Shandong, China.

5 Corresponding Author:

6 Zhen Hu

7 *No. 27 Shanda South Road, Jinan, Shandong 250100,China*

8 E-mail: huzhen885@sdu.edu.cn

9 **Table 1.** Environmental characteristics of the sample sites.

Sample sites	Geographic coordinates	Temperature (℃)	pH	Ammonium (mg N/kg dry sed)	Nitrite (mg N/kg dry sed)	Nitrate (mg N/kg dry sed)	Salinity (‰)
PF	N36° 41', E116° 54'	17	7.3	10.34	0.75	26.97	1.8
CF	N37° 44', E115° 40'	15	7.0	2.627	0.37	46.44	1.1
EC	N36° 40', E117° 03'	32	7.0	0.125	14117.65	941.18	1.2
WS	N36° 42', E117° 02'	22	7.6	815.88	127.19	735.29	2.1

10

11

12

Figure 1

FISH image of the collected samples.

Fig. 1- FISH image of the collected samples. The *M. oxyfera* bacteria was hybridized with probe S-*-DBACT-1027-a-A-18(Cy3, red) and total bacteria was hybridized with probes EUB I-III (FITC, green). a&e, PF; b&f, CF; c&g, EC, d&h, WS. The scale bar indicates 100 μm.

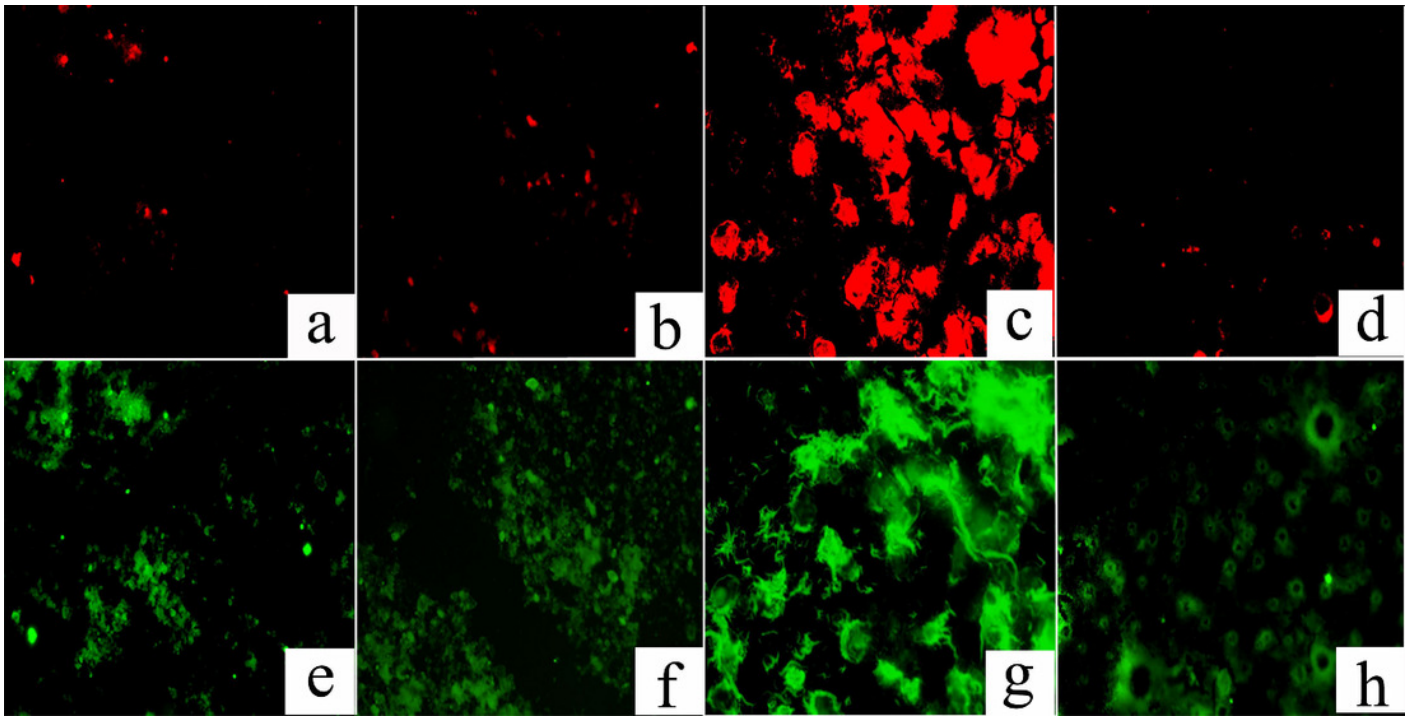

Figure 2

Q-PCR Image of *M. oxyfera* bacteria

Fig. 2- The abundance of *M. oxyfera* bacteria 16S rRNA gene copy numbers of collected samples.

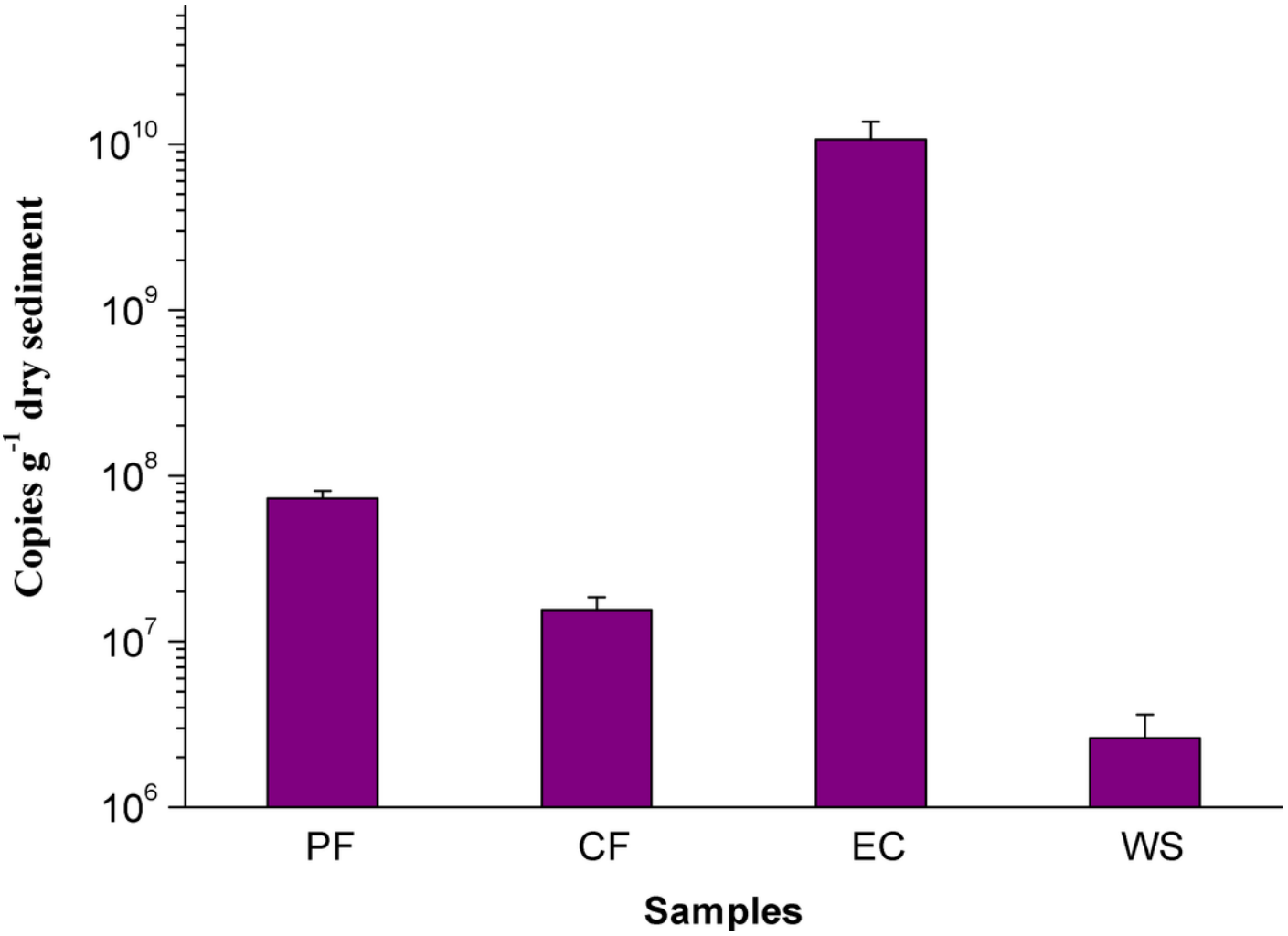

Figure 3

Image of batch test

Fig. 3 The consumption rates of methane and nitrite in the paddy field (a), corn field (b), n-damo enrichment culture (c), WWTP (d).

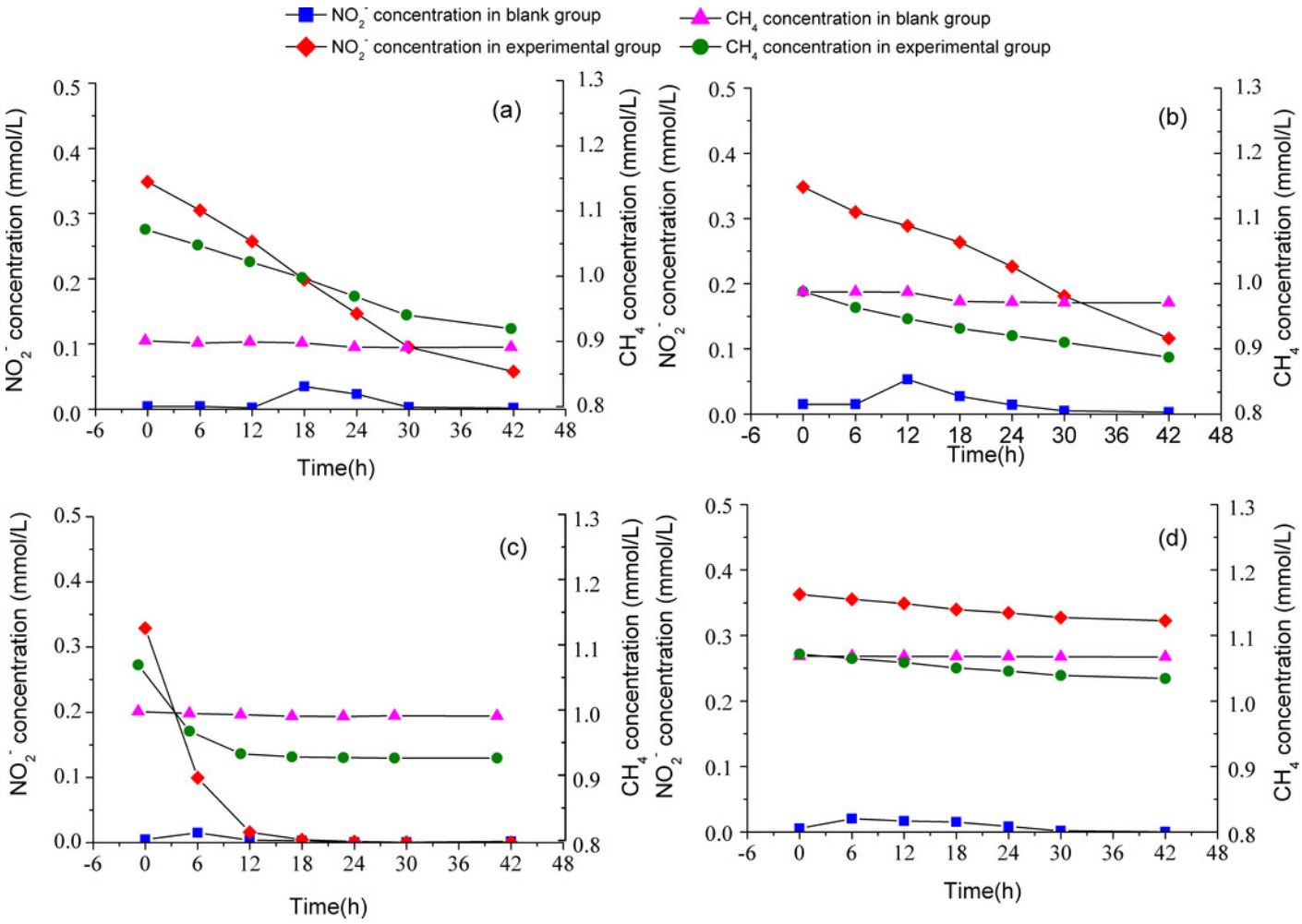

Figure 4

Composition of microbial community

Fig. 4 - Composition of microbial community at phylum level in different samples.

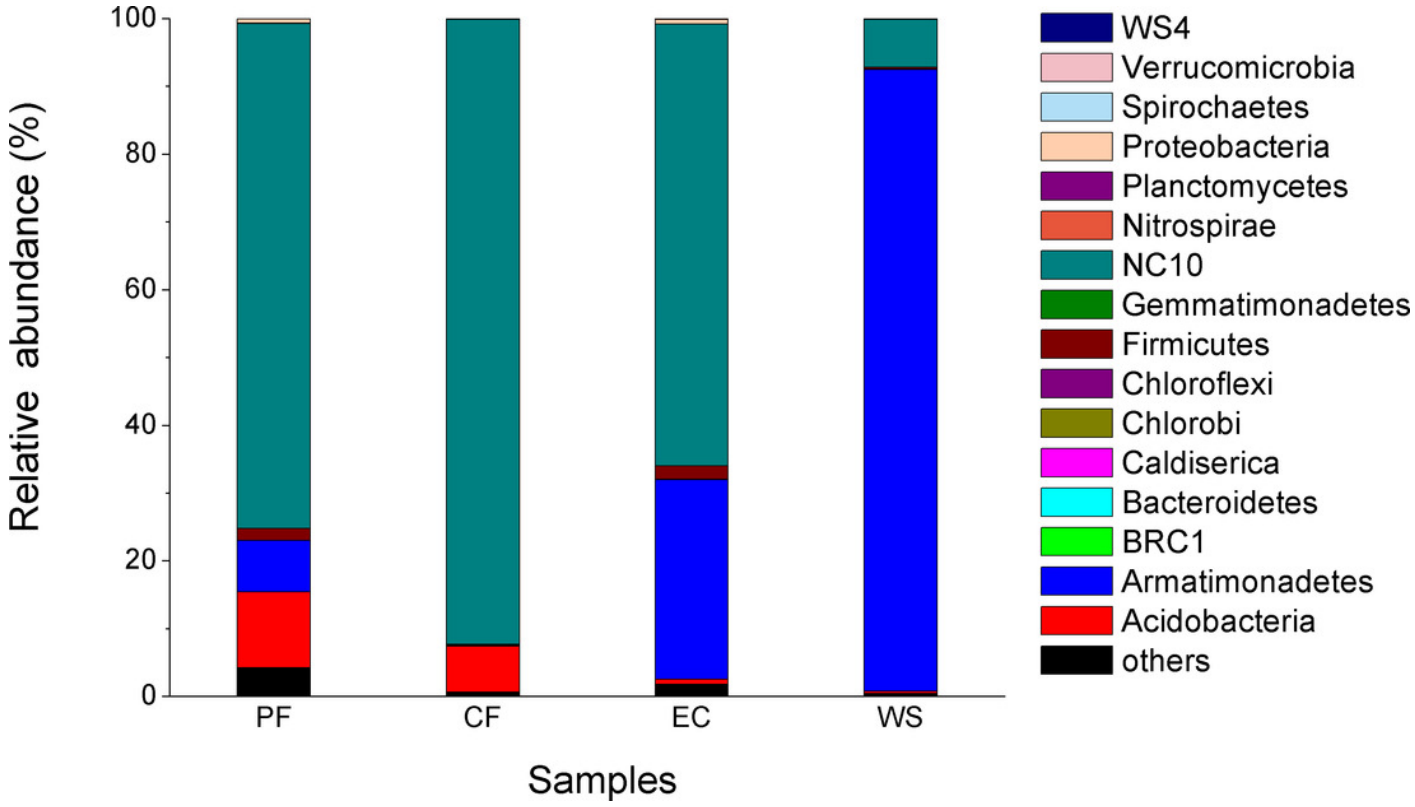

Figure 5

Richness heat map

Fig. 5 - Richness heat map of the 25 most abundant genera.

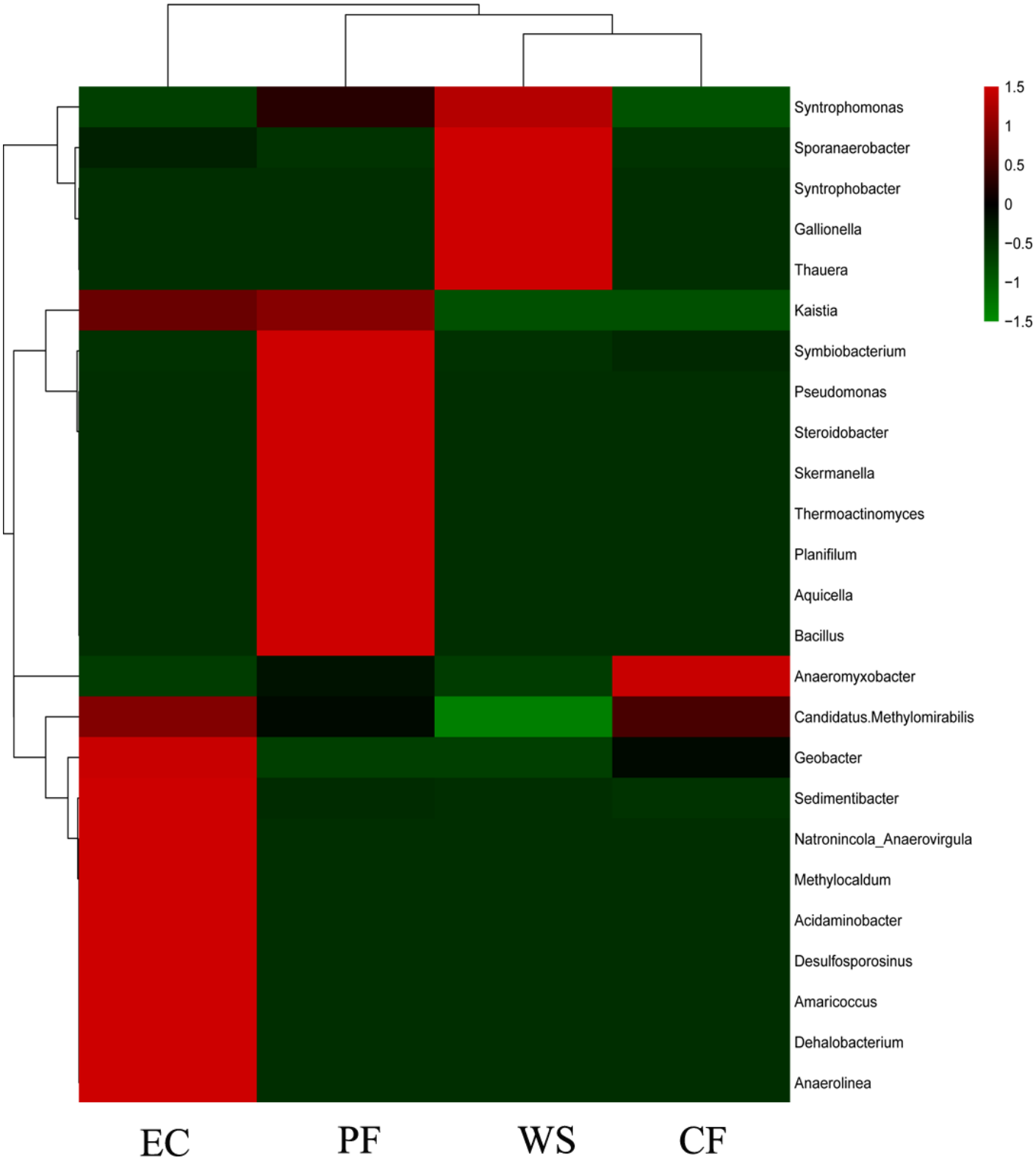
Syntrophomonas
Sporanaerobacter
Syntrophobacter
Gallionella
Thauera
Kaistia
Symbiobacterium
Pseudomonas
Steroidobacter
Skermanella
Thermoactinomyces
Planifilum
Aquicella
Bacillus
Anaeromyxobacter
Candidatus.Methylomirabilis
Geobacter
Sedimentibacter
Natronincola_Anaerovirgula
Methylocaldum
Acidaminobacter
Desulfosporosinus
Amaricoccus
Dehalobacterium
Anaerolinea
1.5
1
0.5
0
−0.5
−1
−1.5
EC
PF
WS
CF